Tracking of individual nanocrystals using diffracted x rays

Y. C. Sasaki,[1,2,*] Y. Suzuki,[1] N. Yagi,[1] S. Adachi,[3] M. Ishibashi,[4] H. Suda,[5] K. Toyota,[6] and M. Yanagihara[6]
[1]*Experimental Division, Japan Synchrotron Radiation Research Institute (JASRI), Spring-8,1-1-1 Kouto, Mikazuki-cho, Sayou-gun, Hyogo 679-5198, Japan*
[2]*Unit Process and Combined Circuit, PRESTO, Japan Science and Technology Corporation, Osaka 565-0082, Japan*
[3]*The Institute of Physical and Chemical Research (RIKEN), Hyogo 679-5143, Japan*
[4]*Advanced Research Laboratory, Hitachi Ltd., Saitama 350-0395, Japan*
[5]*Department of Biological Science and Technology, Tokai University, 317 Nishino, Shizuoka 410-0321, Japan*
[6]*Research Institute for Scientific Measurements, Tohoku University, Sendai 980-8577, Japan*
(Received 22 November 1999)

We demonstrated dynamical observation of an individual nanocrystal in supercooled liquid water with the guidance of x-ray diffracted spots from the nanocrystal itself. This new system, which we call diffracted x-ray tracking, monitored small Brownian motions ($D=0.68$ mrad^2/s at 233 K) of a single nanoparticle in real time and real space.

PACS number(s): 66.20.+d, 07.85.Qe, 61.10.−i

I. INTRODUCTION

Most x-ray experiments are based on the averaged observations of many molecules, so the behavior of each molecule cannot be determined. Nevertheless, in the wavelength region of visible light, recent advances in single molecule detection using optical imaging and spectroscopy have made it possible to investigate individual molecular properties at ambient conditions [1–5]. In this work, we demonstrated direct observation of the rotating motion of an individual nanocrystal in supercooled liquid water using time-resolved Laue diffraction. The principle of individual nanocrystal detection with diffracted x rays consists of monitoring the behavior of each nanocrystal with the guidance of diffracted x-ray spots from the nanocrystal itself. This new system, which we call diffracted x-ray tracking (DXT), monitored the rotational Brownian motion of a single nanoparticle.

In this work, we observed the dynamics of nanocrystals in supercooled liquid water. To understand static and kinetics structures and properties of liquid, the viscosity is of central importance. Values of the viscosity can be determined from motions of diffracted x-ray spots from individual nanocrystals in supercooled liquid water. The viscosity has been measured by a variety of methods, for instance relaxation time measurements in nuclear magnetic resonance and electron spin resonance, and inelastic neutron scattering [6]. Recent studies have directly observed Brownian motions of individual molecules or particles using systems for single molecule detection [7–9]. The relationship between the microscopic viscosity and diffusional motions of molecules is derived by the Stokes-Einstein equation $D=kT/6\pi\eta r'$, where D is diffusion constant, k is Boltzmann's constant, T is the absolute temperature, η is the solvent viscosity, and r' is the molecular radius. In the systems for the optical single-molecule detection, values of D have been determined from three-dimensional or two-dimensional trajectories for individual molecules using the integrated signal from individual bright spots from successive frames [7,8]. DXT can monitor not the position of individual molecules but the rotary motion of individual particles with the guidance of diffracted x-ray spots from the particle itself as shown in Fig. 1(a).

II. PRINCIPLE

In two-dimensional motion, $D=(\Delta z^2)/(4\Delta t)$, where (Δz^2) is the two-dimensional mean square displacement for time lags $\Delta t=(t_i-t_j)$, and $(\Delta z^2)=(1/\Sigma_{\Delta t=(t_i-t_j)})\Sigma_{\Delta t=(t_i-t_j)}(z(t_i)-z(t_j))^2$, where $z(t_i)$ represents the position of the molecule at time t_i [10,11]. In DXT, the relationship between the observed diffraction angle $\Delta\theta$ and the displacement (Δz^2) is $(\Delta\theta^2)r^2=(\Delta z^2)$, where r is the distance from the rotary center as shown in Fig. 1(a). Therefore, the values of $\Delta\theta$ obtained from our DXT can be converted into the values of Δz. When the rotational motion for short times regarded as Brownian motion on a two-dimensional flat surface, the values of D can be determined from DXT. When the observed particles have the radius r' and are located at the distance r [Fig. 1 (a)] of the particle from the rotary center, the relationship $(\Delta\theta^2)r^2/(4\Delta t)=kT/6\pi\eta r'$, applies in the Stokes-Einstein equation. In Stokes' law, it is assumed that the particles are sufficiently distant from boundary walls for the surrounding fluid to be regarded as unbounded. However, in this case, the observed particles were bounded to the polymer rods. According to the simplification of the Navier-Stokes equations [12], the hydrodynamics in this system can be accounted for by replacing r' with r. From this relationship, we can compare DXT with other optical single molecular systems, for example single particle tracking (SPT) [9,10]. The values of η are represented as follows: in the DXT

$$\eta_{\text{x-ray}}=4\Delta tkT/(6\pi r^3(\Delta\theta^2)), \tag{1}$$

and in the SPT

$$\eta_{\text{optical}}=4\Delta tkT/(6\pi r(\Delta z^2)). \tag{2}$$

*Corresponding author. Email address: ycsasaki@spring8.or.jp

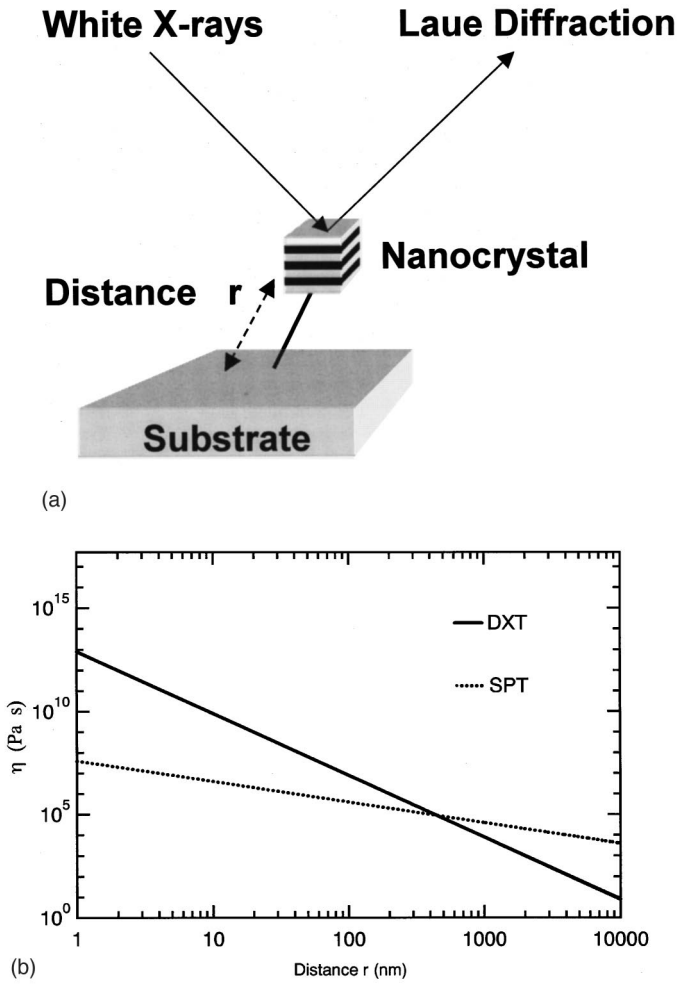

FIG. 1. (a) Schematic drawing of the detection system for single particle tracking with x rays (not to scale). Diffracted x-ray tracking (DXT) monitors the motion of a single particle with the guidance of a diffraction spot from an individual particle (Si/Mo multilayer nanocrystal). The detectable displacement is dependent on the distance *r* between the particle and the rotating center. (b) Comparison between DXT and other systems for single molecular detection, for example, single particle tracking (SPT) by measuring the viscosity of the supercooled liquid water.

Although the SPT monitors the central position of individual particles, the DXT can monitor not the position of individual molecules but the rotating motion of individual particle with the guidance of diffracted x-ray spots from the particle itself.

Direct observations of the kinetic motions of individual water molecules need to understand the nature of supercooled liquid water between 273 and 136 K [13]. In this region, the viscosity of a liquid water grows sufficiently large to 10^{13} Pa s. We examined the possibility of kinetic observations from both $\eta_{\text{x-ray}}$ and η_{optical}. The calculated lines in Fig. 1(b) were assumed as follows: $\Delta t = 1$ s, $T = 136$ K, $(\Delta\theta^2) = 0.05$ mrad^2, and $(\Delta z^2) = 0.01$ nm^2. In DXT, the viscosity of $\sim 10^{13}$ Pa s can be monitored when the distance *r* is approximately 1 nm. However, the limitation of other single molecular systems is on the order of 10^7 Pa s even when the distance *r* is approximately 2 nm. The very high resolution of the DXT, which is not obtainable by the SPT, rests on the strong dependence of the diffraction angle under Laue conditions.

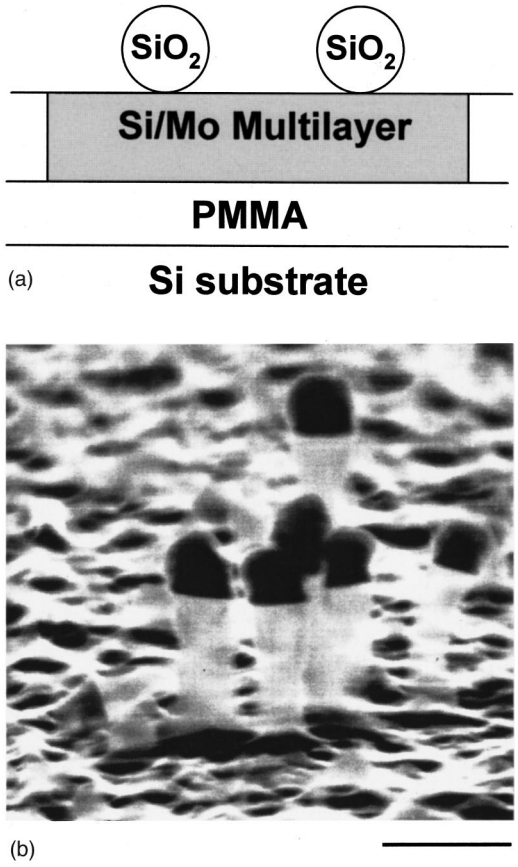

FIG. 2. (a) Cross-sectional view of the fabricated substrate to make the artificial nanocluster. Silicon dioxide beads (Hipresica; Ube-Nitto Kasei, Co. Ltd.) were used as a model protective coating array because the rate of the reactive ion etching with SiO_2 is much lower than that of the Si/Mo multilayer. The diameter of the SiO_2 beads is about 0.1 μm. A thin polymer (polymethylmethacrylate: PMMA) film was used to separate the Si/Mo multilayer from the silicon substrate. (b) Scanning electron micrograph of the Si/Mo cluster on the Si substrate after the reactive ion etching (RIE). Although the etching rate of SiO_2 with oxygen is smaller than that of the Si/Mo multilayer, there is no SiO_2 beads on the Si/Mo multilayer. The black part is assigned to the nanocluster of the Si/Mo multilayer. The scale bar at the bottom right shows 200 nm.

In order to demonstrate the very high resolution of the DXT, we determined the viscosity ($\eta \sim 10^{-3}$ Pa s) of a supercooled liquid water in the region between 273 and 233 K. According to Fig. 1(b), we can detect the motions of a supercooled liquid water using x rays when the value of *r* and $(\Delta\theta^2)$ are ~ 10 μm and ~ 50 mrad^2, respectively. Here, we used the polymer local chain in the beaded agarose gel containing a pure liquid water. Many gels are flexible and have a random coil structure. However, there is a large class of gels which are not flexible and assume a rodlike structure. For example, agarose gels form the helix structure which can be regarded effectively as a rigid rod [14].

III. EXPERIMENT

We used the cluster of an artificial crystal, we call the multilayer (silicon/molybdenum) nanocluster, because many nanoparticles are not perfectly crystallized. Thus, we can

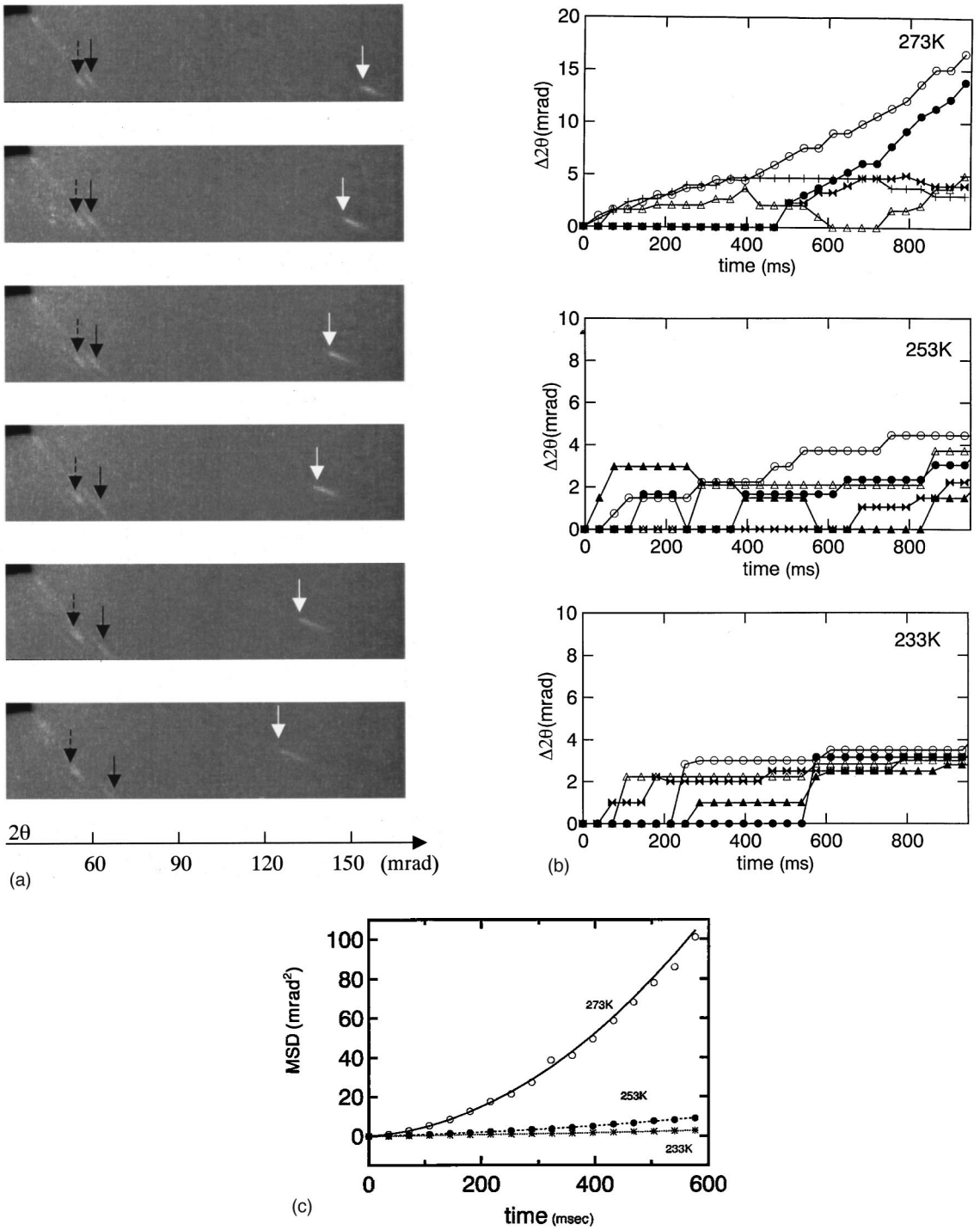

FIG. 3. (a) Six successive expanded images of Laue spots moving in position from frame to frame at 273 K. Frames from (a) to (f) are spaced at 183 s intervals. The exposure time was 36 ms. The Laue spots from individual Si/Mo clusters appeared as brightly shinning dots (white). To show this movement clearly, three spots were labeled by arrows. The direct x-ray beam is located at the upper left side. The averaged exposure time was 36 ms. (b) Motions ($\Delta 2\theta$) of representative nanoclusters (five particles) along the direction of the diffraction angle at each temperature. (c) The mean square displacements ($\Delta\theta^2$) of nanoclusters as a function of time interval Δt at each temperature. The value of D was determined from these fitting curves at each temperature.

continuously detect displacements of individual diffracted spots using the Laue condition. The number of diffracted spots enables us to determine the number of observed nanocrystals because individual multilayer nanoclusters reflect only a single x-ray diffraction spot. In this experiment, we chose both lattice constants and the stacking period ($d = 4$ nm, 20 pairs) for the Si/Mo multilayer [15]. The total thickness of the Si/Mo multilayer is 80 nm. We confirmed this value of total thickness using electron scanning microscopy and x-ray reflectometry. The nanoclusters for the artificial crystals were fabricated by a sequential process using a silicon substrate, silicon dioxide (SiO_2) beads, and microelectronic processing techniques, including reactive ion etching (RIE) as shown in Fig. 2. This sample was etched by RIE

TABLE I. Experimental results. The values of D and v were determined from the plots [Fig. 3(c)] of $(\Delta\theta^2)$ vs the interval times by χ^2 minimization fit for Eq. (3). These values were 63.8% data reliable. The measured spots are about 50 trajectories. The calculated values of η are obtained from Eq. (1). The values of $\eta_{\#}$ are cited from Ref. [15].

Temp. (K)	D (mrad^2/s)	v (mrad/s)	η (Pa s)	$\eta_{\#}$ (Pa s)
293	7.7 ± 0.3	$(1.9\pm0.2)\times10^{1}$	1.0×10^{-3}	1.00×10^{-3}
273	5.1 ± 0.4	$(1.6\pm0.1)\times10^{1}$	1.8×10^{-3}	1.80×10^{-3}
253	1.7 ± 0.2	4.0 ± 0.3	4.5×10^{-3}	4.36×10^{-3}
238				1.87×10^{-2}
233	$(6.8\pm0.9)\times10^{-1}$	1.9 ± 0.4	1.9×10^{-2}	

with a mixture of carbon fluoride and oxygen gasses (CF_4:O_2=9:1) at 100 mW/cm^2 and 7 Pa for 420 s. To fix the Si/Mo clusters in the gel, we used chemical coupling between the carboxyl groups (COOH) in the local chain of the gel and the amino groups (NH^2), which were placed on the surface of the Si/Mo clusters with silane coupling reagent. The Si/Mo clusters were immersed in 10 mM aqueous solution of aminosilane [3-(2-aminoethylaminopropyl) trimethoxysilane] for 1 h. After the aminosilane immersion, the sample was placed in a 110 °C oven for 10 min, and rinsed in the distilled water by filtration (Ultrafree C3, UFC3TTK, Millipore). The amino groups on the Si/Mo clusters can react with the carboxyl groups (COOH) in the local chain of the beaded gel (epoxycarboxyhexmethylamine Sepharose 4B, Pharmacia Biotech). The particle size of the beaded gel in the wet condition is approximately 40–290 μm (agarose concentration 4%). The sample was prepared by incubating the treated Si/Mo cluster in a 10 mM phosphate buffer (pH=6.0) containing 10 mM 1-ethyl-3-(3-(dimethylaminopropyl) carbodiimide hydrochloride (Dojindo Lab.) for 24 h at room temperature, and rinsed in distilled water by filtration (Ultrafree C3, UFC3TTK, Millipore). The agarose gel, which was linked with the Si/Mo clusters, was mounted in thin glass capillaries (typically 0.5 mm inner diameter) at 293 K. We controlled the temperature of the sample capillary with a cryostat using liquid nitrogen and dry air. The temperature of the samples was fixed at 293, 273, 253, and 233 K.

We used the white x-ray mode (Laue mode) of a beamline BL44B2 (RIKEN Structural Biology II, SPring-8, Japan) to record Laue diffraction spots from nanocrystals in thin glass capillaries [16]. Photon flux at the sample position was estimated to be about 10^{15} photon/s/mm^2 in the energy range of 7–30 kV. The x-ray beam's focal size was 0.2 mm (horizontal)$\times$0.2 mm (vertical). A diffraction spot was monitored with an x-ray image intensifier (Hamamatsu Photonics, V5445P) and a charge-coupled device (CCD) camera (Hamamatsu Photonics, C4880-82) with 656$\times$494 pixels. The averaged exposure time was 36 ms. The detector's effective size was 150 mm in diameter with 310 mm sample-to-detector distance.

IV. RESULTS AND DISCUSSION

Figure 3(a) shows six successive expanded images of Laue spots from individual Si/Mo clusters at 273 K. According to the Bragg equation ($2d\sin\theta=n\lambda$), the order of the recorded diffracted spots is $n=3$, 4, 5, and 6, because the value of $2d$ for the Si/Mo multilayer is 8 nm, and the region of x-ray wavelength is $\lambda=0.04-0.18$ nm. We observed these spots moving in all directions from frame to frame. Figure 3(b) shows motions of representative nanoclusters (five particles) along the direction of the diffraction angle at each temperature. Many spots moved randomly along the direction of the diffraction angle. The number of the observed nanoclusters is $\sim$50 particles at each temperature.

The Laue spots from Si/Mo clusters are broadened because of the cluster's small size. According to the theory of Fraunhofer diffraction [17], the half width of the Laue spots $\Delta(2\theta)$ should be measured approximately as $\Delta(2\theta)/(2\theta)\sim2\lambda/2r'$, where λ is the wavelength of the diffracted x ray, $2r'$ (=80 nm) is the effective size (diameter) of the Si/Mo cluster, and 2θ is the diffraction angle. In this experiment, the value of $\Delta2\theta/2\theta$ is estimated to be about 2.8×10^{-2}. This value is in fair agreement with the averaged observed values ($\sim3\times10^{-2}$) of 50 different Laue spots at 233 K. The observed intensity (1000–1500 counts/36 ms) can be converted into the x-ray intensity using the conversion gain (6.5×10^{-2} analog to digital converter unit/photon at 12.4 keV) of the CCD camera. The calibrated x-ray intensity with individual Si/Mo clusters is $\sim5\times10^{5}$ photon/s/cluster. This value is in fair agreement with the calculated value obtained from the photon flux, x-ray reflectivity of the nanocrystal, and size of it.

Figure 3(c) shows the mean square displacement $(\Delta\theta^2)$ of the nanocluster as a function of time interval Δt at each temperature. In simple Brownian diffusion the $(\Delta\theta^2)-\Delta t$ plots are linear with a slope of $4D$, where D is the two-dimensional diffusion coefficient. The simple diffusion mode can be expressed as $(\Delta\theta^2)r^2=4D(\Delta t)$. However, the $(\Delta\theta^2)-\Delta t$ plots are parabolic in these results. This relationship is known as directed diffusion mode [10,11]: $(\Delta\theta^2)r^2=4D(\Delta t)+v^2(\Delta t)^2$. This shows that particles move in a direction at a constant drift velocity v with a diffusion coefficient of D. As expected for directed Brownian motion, a parabolic increase of $(\Delta\theta^2)$ with Δt is found for ensemble average with $D_{293\,\mathrm{K}}$: $D=7.7\pm0.3$ mrad^2/s and $v=(1.9\pm0.2)\times10^{1}$ mrad/s at 293 K as shown in Table I. We determined the value of r from both $D_{293\,\mathrm{K}}$ and the known value of the viscosity (1.0×10^{-3} Pa s) of water at 293 K. If the obtained value of r is equal to the radius r' of the particle, we may expect that the rotary center in this system is located at the point of the rigid rod nanoparticle. In other words, this may show that the rod-particle combination is not rigid but soft. If the obtained value r is larger than that of the radius r'

of the particle, we may expect that the rod-nanoparticle combination is more rigid than the rotary center in the polymer rod (gel). The obtained value of r was 30 μm. As a result, the obtained value of r is larger than that of the radius r' of the nanoparticle in this case. Thus, we mentioned that there is a rotary center at the substrate-rod connection. Thus, we can determine the viscosity of a supercooled liquid water at other temperatures. These values of the viscosity are in fair agreement with known ones (Table I) [18].

We have shown that DXT can monitor the trajectories of individual nanocrystal in real time and real space. The viscosity of supercooled liquid water at atmospheric pressure below 273 K can be monitored to control the distance r between the nanocrystal and the rotary center when molecules bound to nanocrystals do not have conformational changes of structures in these conditions. If this molecule has structural changes, DXT can be immediately utilized for detecting conformational changes of single molecular units. In addition, DXT is available for microscopic measurements of the viscosity in special locations, for example, the surface or interface of molecules and proteins [19].

ACKNOWLEDGMENTS

We thank H. Yamanashi for the Si/Mo cluster, O. Mishima, H. Takei, H. Nishida, Y. Hirai, T. Oka, and H. Iwamoto for discussion, and the staff of Tokyo Electronics and Mechanics Co. for technical support.

[1] Th. Basche, W. E. Moerner, M. Orrit, and U. P. Wild, *Single Molecule Optical Detection, Imaging, and Spectroscopy* (Wiley, Munich, 1997).
[2] T. Funatsu *et al.*, Nature (London) **374**, 555 (1995).
[3] H. Noji, R. Yasuda, M. Yoshida, and K. Jr. Kinosita, Nature (London) **386**, 299 (1997).
[4] S. Weiss, Science **283**, 1676 (1999).
[5] J. K. Gimzewski and C. Joachim, Science **283**, 1683 (1999).
[6] T. DeFries and J. Jonas, J. Chem. Phys. **66**, 896 (1977).
[7] Th. Schmidt *et al.*, Proc. Natl. Acad. Sci. USA **93**, 2926 (1996).
[8] R. M. Dickson, D. J. Norris, Y. Tzeng, and W. E. Moerner, Science **274**, 966 (1996).
[9] J. Gelles, B. J. Schnapp, and M. P. Sheetz, Nature (London) **331**, 450 (1988).
[10] H. Qian, M. O. Sheetz, and E. L. Elson, Biophys. J. **60**, 910 (1991).
[11] A. Kusumi, Y. Sako, and M. Yamamoto, Biophys. J. **65**, 2021 (1993).
[12] J. Happel and H. Brenner, *Low Reynolds Number Hydrodynamics*, 2nd rev. ed. (Martinus Nijhoff, Dordrecht, 1973, fourth printing, 1986).
[13] S. Sastry, Nature (London) **398**, 467 (1999); K. Ito, C. T. Moynihan, and C. A. Angell, *ibid.* **398**, 492 (1999).
[14] S. Arnott *et al.*, J. Mol. Biol. **90**, 269 (1974).
[15] H. Okada *et al.*, Appl. Opt. **33**, 4219 (1994).
[16] S. Adachi, T. Oguchi, and T. Ueki, SPring-8 Annual Report 239, 1996 (unpublished).
[17] M. Born and E. Wolf, *Principles of Optics*, 6th ed. (Pergamon, New York, 1980).
[18] Yu. A. Osipov, B. V. Zheleznyi, and N. F. Bondarenko, J. Phys. Chem. **51**, 748 (1977).
[19] J. V. Alsten and S. Granick, Phys. Rev. Lett. **61**, 2570 (1988).